

Article ID: 1001-3555 (2012) 03-0216-09

Synthesis of Cobalt Doped Mesoporous Silica with high Cyclohexanone Selectivity for Catalytic Oxidation of Cyclohexane by the wild Sugarcane-grass Stems Bio-template Route

QIN Yun^{1,2}, YAO Wen-hua^{1,2}, LI Jun-jie¹, ZHENG Kai¹, ZHANG Xin¹,
WANG Wei^{1*}, WANG Jia-qiang^{1*}

(1. Department of Applied Chemistry, Key Laboratory of Medicinal Chemistry for Natural Resource, Ministry of Education, Yunnan University, Kunming 650091, China;

2. Department of Resources and Environmental, Baoshan College, Baoshan 678000, China)

Abstract: Cobalt doped mesoporous silica (M-Co/SiO₂) was synthesized by using wild sugarcane-grass (*Erianthus rockii*) stems as template and used for the oxidation of cyclohexane. The catalyst was characterized by a combination of various physicochemical techniques, such as X-ray diffraction, N₂ physisorption, diffuse reflectance UV-vis, FT-IR, Scanning electron microscopy. The XRD and N₂ physisorption results indicated that the catalyst was a mesoporous structure material that cobalt oxides were highly dispersed on the surface of the catalyst. The UV-vis result indicated that the presence of both Co²⁺ and Co³⁺. The catalytic oxidation of cyclohexane results exhibited high product (cyclohexanone) selectivity (76.7%) and reasonable substrate conversion (71.0%). The recycling experiment indicated that the catalyst can be reused three times with catalytic activity changed little.

Key words: cobalt doped mesoporous silica; biotemplate; wild sugarcane-grass stems; characterization; selective oxidation of cyclohexane; cyclohexanone

CLC number: O643.3

Document code: A

Biological templates have attracted considerable attention for the syntheses of inorganic materials in the recent several years^[1], because they are generally performed under mild conditions, it is energy-conserving, green, and has little requirement for equipments^[2-8]. Moreover, most natural templates and building blocks can be harvested in large amounts at low costs, thus biomorphic assembly is cheap compared with conventional assembly methods to form nanostructures^[7]. However, the catalytic (except for few photocatalytic) properties of these materials were seldom explored. For example, biomorphic self-supporting MFI-type zeolite frameworks

with hierarchical porosity and complex architecture were prepared using a biological template (Luffa sponge) as macroscale sacrificial structure builder^[2]. Interestingly, the as-synthesized biomimetic ZSM-5 replica showed catalytic activity for cracking of n-hexane with no need for ion-exchange. In our group cobalt doped porous titania-silica was synthesized by using rice husks as both silicon source and template and it presented good product (4-pyridinecarboxylic acid) selectivity (91%) and high substrate conversion rate (96%) for the catalytic oxidation of 4-methyl pyridine^[8].

Cyclohexane oxidation is an important commercial

Received date: 2011-12-21; **Revised date:** 2012-04-26.

Foundation item: The project was supported by the National Natural Science Foundation of China (200863009, U1033603), Natural Science Foundation of Yunnan Pro-vince (2008CD065), Specialized Research Fund for the Doctoral Program of Higher Education and Program for Innovative Research Team (in Science and Technology) in University of Yunnan Province (IRSTYIN), Science Research Fund of Department of Education of Yunnan Province (09Y0462).

Biography: QIN Yun, born in 1960, Bachelor of Science, Associate professor.

* **Corresponding author:** Tel: +86-871-5031567; Fax: +86-871-5031567; Email: jqwang@ynu.edu.cn (J. Wang).

reaction to produce cyclohexanone, which is a starting material used in the production of nylon-6 and nylon-66^[9,10]. Although homogeneous systems have been used for these processes, recent articles have illustrated the use of mesoporous solids including the titanosilicate TS-1, transition metal (Cr, V, Co, Ti, etc.) doped MCM-41^[11] and Mo-MCM-41^[12] for the selective oxidation of this hydrocarbon. In particular, Sakthivel and Selvam used Cr-MCM-41 catalyst for oxidizing cyclohexane, giving a conversion rate of 98.9% with a selectivity of 92.9% towards cyclohexanol.^[13] We showed that cerium doped MCM-41 has achieved very good conversions of 94.6% oxidizing cyclohexane and 82.4% cyclohexanol^[14]. Recently, Ag-substituted anatase phase nano-TiO₂ have been synthesized and used for the selective photocatalytic oxidation of cyclohexane to cyclohexanone^[15]. More recently, in our group cobalt doped SBA-3 was synthesized and found that it exhibited high cyclohexane conversion (91.6%) and reasonable product (cyclohexanone) selectivity (64.3%)^[16]. Interestingly, incorporation of 4-(methylamino)benzoic acid together with chromium into the rice husk silica framework gave 100% conversion of cyclohexane in a much shorter time^[17]. Biomimetic iron(III) complexes immobilized within nano-reactors of Al-MCM-41 exhibited excellent activity for the production of cyclohexanone^[18]. Although considerable efforts have been made, cyclohexane oxidation continues to be a challenge^[19].

Wild sugarcane-grass stems (*Erianthus rockii*) is a drought and cold tolerant wild relative of sugar cane from China that is currently being used in sugar cane introgression programs^[20]. However, there is no report on using wild sugarcane-grass stems as template so far as we know. Herein, it was used as template or macroscale sacrificial structure builder^[2] to synthesize cobalt doped mesoporous silica (M-Co/SiO₂) which was used as a catalyst for the catalytic oxidation of cyclohexane.

1 Experimental Section

1.1 Materials

Erianthus rockii samples were randomly collected

from a suburb house of Kunming (latitude: 102.7 °N; longitude: 25 °E; altitude: 1 900 m), Yunnan Province, China. Other chemical reagents, such as, tetraethyl orthosilicate (TEOS), 2-propanol, HCl, cyclohexane, cyclohexanone, cyclohexanol, acetic acid and aqueous hydrogen peroxide (H₂O₂, 30%) were of analytical grades and used as received.

1.2 Synthesis of M-Co/SiO₂

The stems of *Erianthus rockii* were washed thoroughly with water to remove the adhering soil and dust. Then they were cut and immersed in 1 mol L⁻¹ HCl solution at 353 K for 48 h to eliminate metallic impurities and washed with distilled water until no Cl⁻ was detected. The stems were further rinsed in 2-propanol repeatedly until they were completely dehydrated. Then 20 mL (0.09 mol) TEOS was dissolved in 50 mL ethanol and the dehydrated *Erianthus rockii* stems were simply dipped into this solution. The samples were shaken in an ultrasonic bath for 3 h to release the air bubbles emanating from the *Erianthus rockii* stems and allow the solution containing TEOS to enter the stems more easily. Subsequently, the cobalt precursor (Co(NO₃)₂·6H₂O) was introduced with Si/Co (molar) ratio of 50. The samples were shaken in an ultrasonic bath for another 3 h and then placed quietly for 12 h. The above solution was added with 10 mL ammonia. After a desired period of time, *Erianthus rockii* stems were filtered out and washed with distilled water to pH 7.5. The treated *Erianthus rockii* stems were dried in air at room temperature and calcined at 823.15 K for 8 h in an oven in air to burn off the organics. After naturally cooling to room temperature, a laurel-green product, M-Co/SiO₂ was obtained.

1.3 Characterizations

X-ray powder diffraction (XRD) experiments were conducted on a D/max-3B spectrometer with Cu Kα radiation, and scans were made in the 2θ range 10° ~ 100° with a scan rate of 10°/min (wide angle diffraction). Pore size distributions, BET surface areas, and pore volumes were measured by nitrogen adsorption/desorption using ASAP2020 gas sorption analyzer (Micromeritics Crop). Prior to the analysis, the samples were degassed at 150 °C for 10 h. UV-vis dif-

fuse reflectance spectra were measured at room temperature in air on a SHIMADZU UV-2401PC photometer over the range from 200 to 800 nm. FT-IR measurements were performed on a Thermo Nicolet 8 700 instrument. Potassium bromide pellets containing 0.5% of the catalyst were used in FT-IR experiments and 32 scans were accumulated for each spectrum in transmission, at a spectral resolution of 4 cm^{-1} . The spectrum of dry KBr was taken for background subtraction. Scanning electron microscopy (SEM) images were taken on a FEIQuanta200FEG microscope at an accelerating voltage of 15 kV with the pressure in the sample chamber of 1 Torr. Inductively coupled plasma atomic emission spectrometry (ICP AES; Labtam Plasma Lab 8 440) analysis was used to determine the content of metal in the catalysts.

1.4 Oxidation of cyclohexane

The oxidation reactions were carried out at the atmospheric pressure as follows: The catalyst (50 mg), cyclohexane (AR grade, 750 mg) and 15 mL of solvent (acetic acid, ethyl acetate, acetonitrile and ethanol were used as received without further purification) were added successively into a temperature-controlled, round bottom, two-necked-flask having a reflux condenser. The aqueous H_2O_2 (30% solution, approximately 5 mL) was added dropwise after the reaction mixture was heated to the set temperature. The reaction mixture was filtered under reduced pressure after the set time. The residue was extracted with diethyl ether. Anhydrous Na_2CO_3 (AR grade) was used to remove more water from the extracted organic phase. Then the mixture was filtered under reduced pressure and washed again by diethyl ether. The obtained products were analyzed by gas chromatography (Shimadzu GC-14C) with a packed column ($3\text{ m} \times \phi 2\text{ mm}$, 10% PEG 20 M/101) and a flame ionization (FID) detector. Reference substances were used for the identification of the products.

2 Results and Discussion

2.1 The characterization of M-Co/SiO₂

Fig. 1 shows wide-angle X-ray diffraction (XRD) patterns of M-Co/SiO₂ measured at 2θ of $10^\circ \sim 100^\circ$.

Wide-angle XRD results showed M-Co/SiO₂ had the characteristic of amorphous silica phase which is consistent with the observation of FT-IR spectra. It is worth noting that no distinct diffractions corresponding to any crystalline cobalt oxides are observed at higher angles. This implies that cobalt oxides were highly dispersed on the surface of the catalyst. Similar observations have been reported for Co-MCM-41 and Co-SBA-3^[15,16].

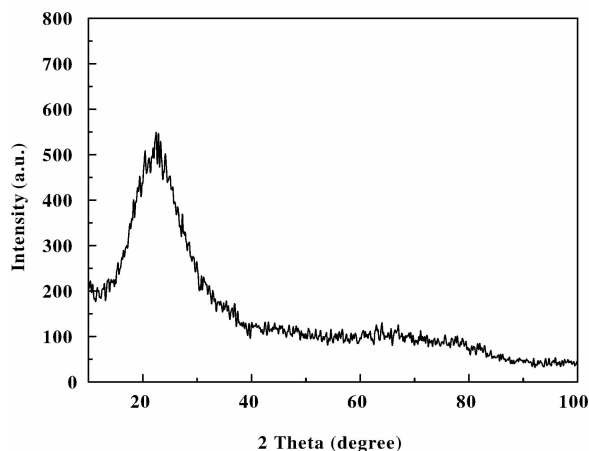


Fig. 1 XRD pattern of M-Co/SiO₂

The N_2 adsorption/desorption isotherms of M-Co/SiO₂ are shown in Fig. 2. The isotherm of M-Co/SiO₂ can be classified as type IV according to the IUPAC convention and is typical of mesoporous structure of prepared material. This is also supported by the big average pore diameter (12.6 nm), BET surface areas ($438\text{ m}^2 \cdot \text{g}^{-1}$), and pore volume ($1.5\text{ cm}^3 \cdot \text{g}^{-1}$). In addition, the BJH pore size distribution of M-Co/SiO₂ (inset in Fig. 2) shows one primary pore size distribution in the mesopores region between 2.1 and 45 nm which indicates that the catalyst has irregular pore channels.

The diffuse reflectance UV-vis spectrum of M-Co/SiO₂ is given in Fig. 3. The absorption at 400 nm indicates the presence of Co^{3+} and the absorption at 500 ~ 800 nm can be attributed to the presence of both Co^{2+} and Co^{3+} [21–23].

The FT-IR spectra of M-Co/SiO₂ and Co-MCM-41 was recorded between 400 cm^{-1} and $4\,000\text{ cm}^{-1}$ in transmission mode and shown in Fig. 4. Obviously, they are very similar. No bands associated with orga-

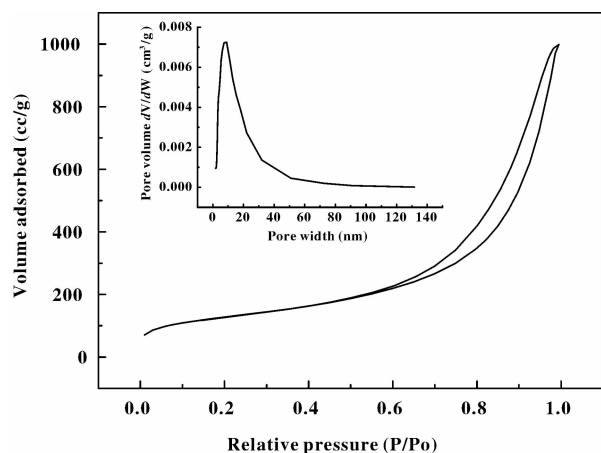


Fig. 2 Nitrogen adsorption/desorption isotherm and BJH pore size distribution of M-Co/SiO₂

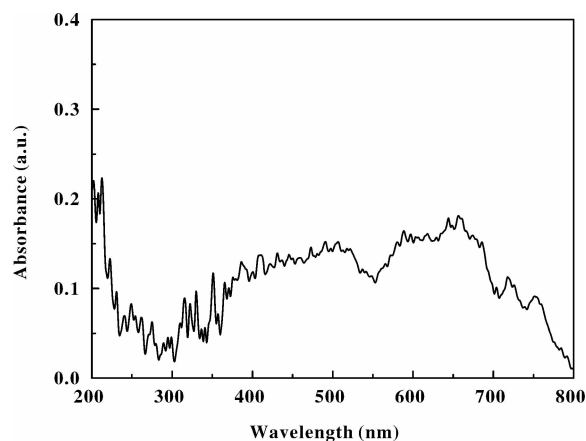


Fig. 3 UV-vis spectra of M-Co/SiO₂

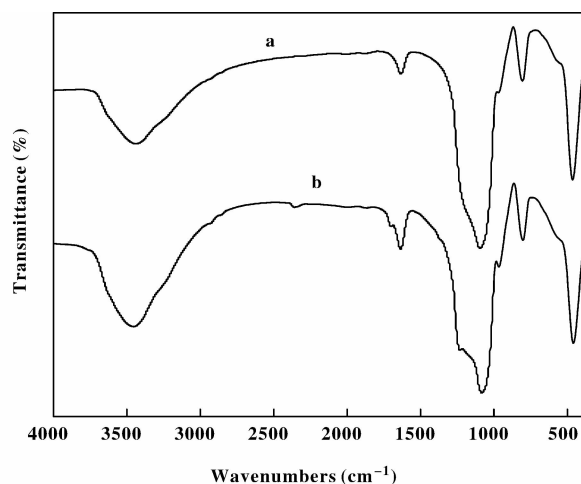


Fig. 4 FT-IR spectra of (a) M-Co/SiO₂ and (b) Co-MCM-41

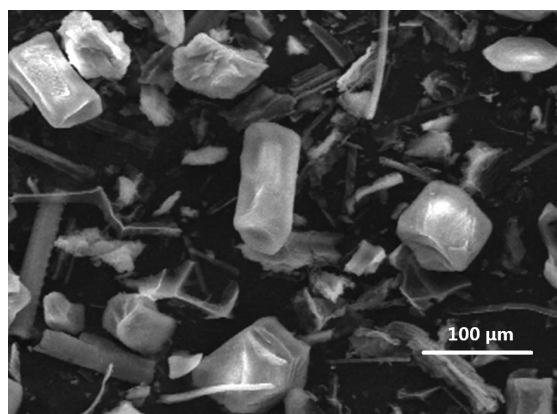


Fig. 5 SEM of M-Co/SiO₂

tics are observed. The bands at ca. 1 090 and ca. 790 cm⁻¹ are due to the asymmetric and symmetric Si-O-Si stretching modes, respectively^[24, 25]. However, after the incorporation of Co into the framework of SiO₂, the shift of the band from 1 080 to 1 105 cm⁻¹ was observed. The shift is bigger than the incorporation of Co into the framework of MCM-41. In the hydroxyl region (3 000 ~ 3 500 cm⁻¹), the broad bands are observed at ca. 3 400 and 3 450 cm⁻¹ for both Co-MCM-41 and M-Co/SiO₂^[26, 27].

SEM image presented in Fig. 5 shows the morphology of M-Co/SiO₂. The hierarchical and complex architecture including cubic, cylindrical and also some irregular shapes with random size at 35 ~ 55 μm was obtained.

The X Ray Fluorescence (XRF) measurement of

M-Co/SiO₂ revealed that molar ratio of Co/Si (molar ratio in the catalysts is 0.007, much lower than that of 0.02 calculated by the amount of Co(NO₃)₂ · 6H₂O and TEOS in the preparing process. This could be caused by the loss of cobalt ions during synthesis.

2.2 Catalytic performance

Using cobalt doped mesoporous silica prepared by above process as a catalyst, it was found that the main products detected are cyclohexanone and cyclohexanol for the oxidation of cyclohexane. Little cyclohexyl acetate could be detected as by-products. Cyclohexyl acetate was possibly produced due to the termination reaction between unreacted cyclohexyl and acetoxy radicals and/or by a possible reaction of cyclohexanol with excess acetic acid in the presence of the catalyst^[28]. The effects of catalysts on the cyclohexane oxidation are shown in Table 1. It is seen that M-Co/SiO₂ has the

reasonable conversion rate of 71.0% , which is significantly higher than Co-SBA-15 , but lower than Co-HM-CM-41^[29] and Co-SBA-3. However, M-Co/SiO₂ has the highest selectivity of (76.7%) compared with Co-HMCM-41, Co-SBA-3 and Co-SBA-15 reported in ref^[16]. Although Co- HMCM-41, Co-SBA-3 and Co-SBA-15 have much bigger surface area than M-Co/

SiO₂ synthesized by using *Erianthus rockii* stems as template, they are less selectivity compared with M-Co/SiO₂. This may imply that pore size would play more important role since the pore size of M-Co/SiO₂ (12.6 nm) is much bigger than Co-HMCM-41, Co-SBA-3 and Co-SBA-15 whose pore size is 2.8 , 3.6 , 4.5 nm, respectively.

Table 1 Effects of catalysts on the cyclohexane reaction^a

Catalysts	Conversion (%)	TON	Selectivity (%)		
			Cyclohexanone	Cyclohexanol	By-product
Co/SBA-3 ¹⁶	91.6	500.3	64.3	35.6	0.1 ^b
Co/SBA-15 ¹⁶	42.8	233.8	68.0	31.8	0.2
Co-HMCM-41 ^{29c}	80.8	91.0	14.2	76.1	9.7
M-Co/SiO ₂	71.0	387.8	76.7	21.2	2.1

^aReaction conditions: reaction time, 10 h; catalyst, 50 mg; reaction temperature, 373 K; ^b Cyclohexyl acetate; ^c Reaction conditions: reaction time, 12 h; catalyst, 400 mg; reaction temperature, 373 K
TON, turn over number (millimole of oxidized products per millimole of metal in the catalyst).

The high efficiency of M-Co/SiO₂ may also be explained as follows: Firstly, the big surface area, high thermal stability and excellent mechanical strength of M-Co/SiO₂ makes M-Co/SiO₂ a highly effective catalyst since the intradiffusion resistance is minimized and the efficiency of selective oxidation is enhanced. Secondly, the results obtained from XRD, FT-IR and diffuse reflectance UV-vis spectroscopy indicate that both Co²⁺ and Co³⁺ are well dispersed on the silica surfaces and is more like that of Co-SBA-3^[16]. These factors can also modify the efficiency. Thirdly, since it also exhibited higher selectivity than Co-SBA-3 and Co-SBA-15 reported in ref. ^[16], its hierarchical porosity and complex architecture including cubic ,cylindrical and also some irregular shapes has an important impact on the catalytic activity. This should also help to overcome the intradiffusional resistance in a typical mesoporous material.

2.3 Effect of reaction temperature

As shown in Fig. 6, the catalytic performances were affected by temperature. The conversion of cyclohexane increased by increasing the reaction temperature and passed through a maximum at 373 K while the

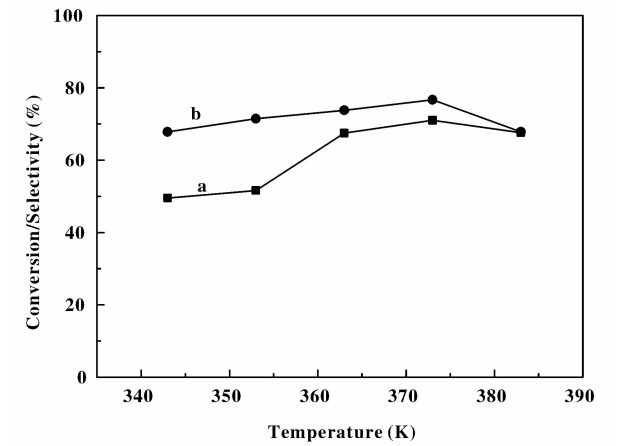


Fig. 6 Effect of reaction temperature on the conversion and selectivity over M-Co/SiO₂
a) Conversion of cyclohexane; (b) Selectivity of cyclohexanone
(Reaction condition: 750 mg cyclohexane, 50 mg catalyst, 15 mL acetic acid, 10 h reaction time)

selectivity to cyclohexanone increased. A further increase in the reaction temperature resulted in decrease both conversion and selectivity, probably owing to a quicker decomposition of H₂O₂ at higher temperature which resulted in a relatively low activity^[14]. Thus, 373 K was chosen as the suitable temperature for the

oxidation of cyclohexane.

2.4 Effect of reaction time

The effect of reaction time on cyclohexane oxidation was also investigated and depicted in Fig. 7. It is seen that the conversion of the cyclohexane increased with time up to 12 h while the selectivity passed through a maximum at 10 h, a further increase in the reaction time resulted in slightly decrease in the selec-

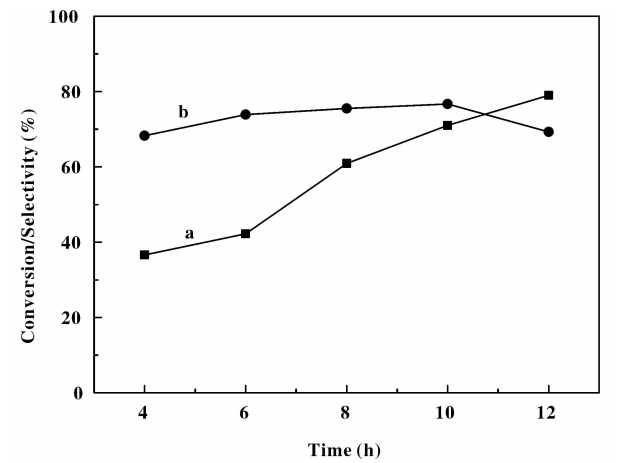


Fig. 7 Effect of reaction time on the conversion and selectivity over M-Co/SiO₂
a) Conversion of cyclohexane; (b) Selectivity of cyclohexanone
(Reaction condition: 750 mg cyclohexane, 50 mg catalyst, 15 mL acetic acid, 373 K for reaction temperature)

tivity of cyclohexanone. Therefore, the optimum conversion and selectivity could be achieved at about 10 h.

2.5 Effect of solvents

The nature of solvents was known to have a major influence on reaction kinetics and product conversion in the oxidation of cyclohexane. Therefore, the effects of various solvents on the reaction are summarized in Table 2. Obviously, M-Co/SiO₂ has the best performance in acetic acid. This is due to possible partial decomposition of H₂O₂ because it was reported that the decomposition of H₂O₂ are faster in these solvent than acetic acid^[30]. Moreover, it has been reported that acetic acid does not only act as a solvent, but also serves as a good oxidizing agent because of the formation of the framework silica peroxy acetic acid complex probably formed in the pores of cobalt doped mesoporous silica, then it would be more hydrophobic and stable, as compared with hydrogen peroxide^[31]. Therefore, a better interaction of this complex with cyclohexane can be expected. In general, it is considered that acetic acid does not only facilitate homogeneity of the liquid phase, but also be responsible for the increase in overall oxidation activity.

Table 2 Effects of solvents on the cyclohexane oxidation^a

Solvents	Conversion (%)	TON	Selectivity(%)	
			Cyclohexanone	Cyclohexanol
Acetic acid	71.0	387.8	76.7	21.2
Ethanol	10.8	59.0	48.3	51.7
Ethyl acetate	10.0	54.6	67.9	32.1
Acetonitrile	13.8	75.4	22.2	23.0

^aReaction conditions: reaction time, 10 h; catalyst, 50 mg; reaction temperature, boiling point of solvents, except for acetic acid at 373 K

2.6 Effect of Co/Si molar ratio

Table 3 showed the effect of cobalt content on the reaction. It is seen that the cyclohexane conversion and cyclohexanone selectivity increased with cobalt content and that a maximum conversion was obtained at Co/Si

ratio of 1/50. However, the observed decrease in cyclohexane conversion and cyclohexanone selectivity at higher cobalt content (Co/Si = 1/30) could be due to the presence of excess amount of cobalt, which lead to competent interaction of metal oxo-species with both al-

kylperoxy species and cyclohexane, thus inhibiting the catalytic oxidation^[32].

Table 3 Effect of molar ratio of Co/Si the cyclohexane oxidation^a

Molar ratio of Co/Si	Conversion (%)	Selectivity(%)	
		Cyclohexanone	Cyclohexanol
1:30	38.3	58	42
1:50	71.0	76.7	21.2
1:70	9.1	17.6	82.4

^a Reaction conditions: reaction time, 10 h; catalyst, 50 mg; reaction temperature, 373 K

2.7 The reusability and fast hot catalyst filtration experiment

To check the stability and recycling ability as well as leaching of cobalt ions from M-Co/SiO₂ under reaction conditions, recycling experiment were carried out using acetic acid as solvent. The typical recycling procedure was as follows: after the initial reaction, the catalyst was separated from the reaction mixture and washed with acetone and dried at 363 K, followed by the activation at 673 K for 4 h. The reaction was then carried out on the recycled activated catalyst under the optimum condition. The results are also summarized in Table 4. The recycling experiment results indicated that the catalyst can be reused three times with catalytic activity changed little. These results indicate that the catalyst is a stable.

Table 4 Recycling experiment of the catalyst under the optimum condition^a

Recycling times	Conversion (%)	Selectivity(%)	
		Cyclohexanone	Cyclohexanol
First	71.0	76.7	21.2
Second	65.1	75.1	22.6
Third	61.7	70.9	23.9

^a Reaction conditions: reaction time, 10 h; catalyst, 50 mg; reaction temperature, 373 K

In order to prove whether M-Co/SiO₂ is a heterogeneous one, experiments with fast hot catalyst filtra-

tion and studying the reactivity of the filtrate had been done by a modified process as described in ref. ^[33]: 50 mg catalyst, 750 mg cyclohexane, 10 mL HAc and a certain amount of H₂O₂ was stirred at the temperature of 373 K for 1 h (conversion of cyclohexane was 0.9%). The observation was also well supported by ICP-AES analysis of the filtrates obtained from the fast hot catalyst filtration where negligible amount of leaching of active cobalt ≤0.002%. These indicated that the active component (cobalt) did not leach to the solution and M-Co/SiO₂ was a heterogeneous catalyst.

3 Conclusions

It can be concluded that cobalt doped mesoporous silica prepared by using *Erianthus rockii* stems as template was an efficient and highly selective catalyst for the oxidation of the cyclohexane to cyclohexanone under relatively mild reaction conditions without adding any initiator. Fast hot catalyst filtration experiment proved that the catalyst acted as a heterogeneous one and it can be reused once with almost the same activity. We believe that the synthetic strategy demonstrated here could be extended to other mesoporous materials and other plants. This could open up new uses for mesoporous silica prepared by using biotemplates in highly selective oxidations.

References:

[1] Crepaldi E L, Soler-Illia A A, Grosso D, *et al.* Controlled formation of highly organized mesoporous titania thin films: from meso-structured hybrids to mesoporous nanoanatase TiO₂[J]. *J. Am. Chem. Soc.*, 2003, **125**: 9 770 – 9 786

[2] Zampieri A, Mabande G T P, Selvam T, *et al.* Biotemplating of luffa cylindrica sponges to self-supporting hierarchical zeolite macrostructures for bio-inspired structured catalytic reactors[J]. *Mater. Sci. Eng. C*, 2006, **26**: 130 – 135

[3] Qian J, Wang J, Hou G, *et al.* Preparation and characterization of biomorphic SiC hollow fibers from wood by chemical vapor infiltration[J]. *Scripta Mater*, 2005, **53**: 1 363 – 1 368

[4] Jorgensen M R, Yonkeea B P, Bartl M H. Solid and hollow inorganic replicas of biological photonic crystals[J].

- Scripta Mater.*, 2011, **65**: 954 – 957
- [5] Huang J G, Kunitake T, Onoue S. A facile route to a highly stabilized hierarchical hybrid of titania nanotube and gold nanoparticle[J]. *Chem. Commun.*, 2004, **8**: 1 008 – 1 009
- [6] Li X, Fan T, Zhou H, *et al.* Enhanced light-harvesting and photocatalytic properties in morph-TiO₂ from green leaf biotemplates [J]. *Adv. Funct. Mater.*, 2009, **19**: 45 – 56
- [7] Fan T, Chow S K, Zhang D. Biomimetic mineralization: from biology to materials [J]. *Prog. Mater. Sci.*, 2009, **54**: 542 – 659
- [8] Zhai Z B, Miao Y C, Sun Q, *et al.* Synthesis of cobalt doped porous titania-silica prepared by using the rice husks as both silicon source and template and its catalytic oxidation of 4-methyl pyridine [J]. *Catal. Lett.*, 2009, **131**: 538 – 544
- [9] Cai Q, Aitken K S, Fan Y H, *et al.* A preliminary assessment of the genetic relationship between *Erianthus rockii* and the “Saccharum complex” using microsatellite (SSR) and AFLP markers [J]. *Plant Science.*, 2005, **169**: 976 – 984
- [10] a. Tao Jia-lin(陶家林), Tang De-jin(唐得金), Li Qing(李庆), *et al.* Cyclohexane oxidation catalyzed by titanium silicalite (TS-1) with hydrogen peroxide [J]. *J. Natural Gas Chem.* (Chinese), 2001, **10**: 295 – 307
b. Mao Zhi-hong(毛志红), Wang Jie(王洁), Li Gui-xian(李贵贤), *et al.* Synthesis of bengalelehyde cycic ethyeic acefal by the H₂PMO₁₀V₂O₄₀ immobilized on silylated dalygorskife [J]. *J. Mol. Catal.* (China) (分子催化), 2011, **25**(5): 393 – 399
- [11] Weissert K, Horpe H J. Industrial Organic Chemistry, 2nd edit., VCH Press, Weinheim [M]. 1993
- [12] Carvalho W A, Varaldo P B, Wallau M, *et al.* Mesoporous redox molecular sieves analogous to MCM-41 [J]. *Zeolites*, 1997, **18**: 408 – 416
- [13] Rana R K, Pulikottil A C, Viswanathan B. Synthesis, characterization and activity of Mo-MCM-41 [J]. *Stud. Surf. Sci. Catal.*, 1998, **113**: 211 – 217
- [14] Sakthivel A, Selvam P. Mesoporous (Cr) MCM-41: a mild and efficient heterogeneous catalyst for selective oxidation of cyclohexane [J]. *J. Catal.*, 2002, **211**: 134 – 143
- [15] Yao W H, Chen Y J, Min L, *et al.* Liquid oxidation of cyclohexane to cyclohexanol over cerium-doped MCM-41 [J]. *J. Mol. Catal. A. Chem.*, 2006, **246**: 162 – 166
- [16] Vinu R, Madras G. Photocatalytic activity of Ag-substituted and impregnated nano-TiO₂ [J]. *Appl. Catal. A.*, 2009, **366**: 130 – 140
- [17] Liu X C, He J, Yang L, *et al.* Liquid-phase oxidation of cyclohexane to cyclohexanone over cobalt-doped SBA-3 [J]. *Catal. Commun.*, 2010, **11**: 710 – 714
- [18] Adam F, Retnam P, Iqbal A. The complete conversion of cyclohexane into cyclohexanol and cyclohexanone by a simple silica-chromium heterogeneous catalyst [J]. *Appl. Catal. A. Gen.*, 2009, **357**: 93 – 99
- [19] Farzaneha F, Poorkhosravani M, Ghandi M. Utilization of immobilized biomimetic iron complexes within nanoreactors of Al-MCM-41 as cyclohexane oxidation catalyst [J]. *J. Mol. Catal. A. Chem.*, 2009, **308**: 108 – 133
- [20] Schuchardt U, Cardoso D, Sercheli R, *et al.* Cyclohexane oxidation continues to be a challenge [J]. *Appl. Catal. A.*, 2001, **211**: 1 – 17
- [21] Brik Y, Kacimi M, Ziyad M, *et al.* Titania-supported cobalt and cobalt phosphorus catalysts: characterization and performances in ethane oxidative dehydrogenation [J]. *J. Catal.*, 2001, **202**: 118 – 128
- [22] Wang J Q, Uma S, Klabunde K. Visible light photocatalysis in transition metal incorporated titania-silica aerogels [J]. *J. Appl. Catal. B.*, 2004, **48**: 151 – 154
- [23] Wang J Q, Uma S, Klabunde K. Visible light photocatalysis activities of transition metal oxide/silica aerogels [J]. *Micropor. Mesopor. Mat.*, 2004, **75**: 143 – 147
- [24] Primeau M, Vautey C, Langlet M. The effect of thermal annealing on aerosol-gel deposited SiO₂ films: a FTIR deconvolution study [J]. *Thin Solid Films.*, 1997, **310**: 47 – 56
- [25] Zelenák V, Hornebecq V, Mornet S, Schäfer O, Llewellyn P. Mesoporous silica modified with titania: structure and thermal stability [J]. *Chem. Mater.* 2006, **18**: 3 184 – 3 191
- [26] Peng T, Zhao D, Song H, Yan C. Preparation of lanthana-doped titania nanoparticles with anatase mesoporous walls and high photocatalytic activity [J]. *J. Mol. Catal. A: Chem.*, 2005, **238**: 119 – 126
- [27] Soler-Illia G, Louis A, Sanchez C. Synthesis and characterization of mesostructured titania-based materials through evaporation-induced self-assembly [J]. *Chem. Mater.*, 2002, **14**: 750 – 759
- [28] Dapurkar S E, Sakthivel A, Selvam P. Mesoporous VMCM-41: highly efficient and remarkable catalyst for selective oxidation of cyclohexane to cyclohexanol [J]. *Mol. Catal. A: Chem.*, 2004, **223**: 241 – 250

- [29] Gao Jian-jun(高建军). Master Dissertation of Yunnan University(云南大学硕士研究生学位论文)[D]. 2009
- [30] Mimoun H, Saussine L, Daire E, *et al.* Vanadium(V) peroxy complexes. new versatile biomimetic reagents for epoxidation of olefins and hydroxylation of alkanes and aromatic hydrocarbons[J]. *J. Am. Chem. Soc.*, 1983, **105**: 3 101 – 3 110
- [31] Sooknoi T, Limtrakul J. Activity enhancement by acetic acid in cyclohexane oxidation using Ti-containing zeolite catalyst[J]. *Appl Catal A*, 2002, **233**: 227 – 237
- [32] Sheldon R, Wallau M, Arends I, *et al.* Heterogeneous catalysts for liquid-phase oxidations: philosophers' stones or trojan horses [J]. *Acc. Chem. Res.*, 1998, **31**: 485 – 493

以野生滇蔗茅为生物模板剂合成 Co 掺杂的介孔 SiO₂ 高选择性催化氧化环己烷制备环己酮

秦 云^{1,2}, 姚文华^{1,2}, 李俊杰¹, 郑 凯¹, 张 新¹, 王 伟^{1,*}, 王家强^{1,*}

(1. 云南大学 应用化学系 教育部自然资源药物化学重点实验室, 云南 昆明 650091;

2. 保山学院 资源环境学院, 云南 保山 678000)

摘 要: 以野生滇蔗茅为生物模板剂合成 Co 掺杂的介孔 SiO₂ 催化氧化环己烷. 并用 X 射线衍射、N₂-物理吸附和解吸附、紫外-可见光光度计、傅里叶红外光谱仪和扫描电镜对材料进行了表征. X 射线衍射、N₂-物理吸附和解吸附研究表明该材料为介孔材料且氧化钴高分散于介孔材料的表面. 紫外-可见光光谱表明钴离子以 Co²⁺ 和 Co³⁺ 的形态存在. 环己烷的催化氧化结果表明催化剂能高效催化环己烷(环己烷的转化率为 71.0%) 转化为环己酮(选择性高达 76.7%). 催化剂的重复性试验表明该催化剂具有较高的稳定性, 循环使用 3 次后, 催化活性仅有微小的改变.

关键词: Co 掺杂介孔 SiO₂; 生物模板; 选择性氧化; 环己烷; 环己酮